We are IntechOpen, the world's leading publisher of Open Access books Built by scientists, for scientists

4,800
Open access books available

122,000
International authors and editors

135M
Downloads

Our authors are among the

154
Countries delivered to

TOP 1%
most cited scientists

12.2%
Contributors from top 500 universities

CLARIVATE ANALYTICS BOOK CITATION INDEX INDEXED

WEB OF SCIENCE™

Selection of our books indexed in the Book Citation Index in Web of Science™ Core Collection (BKCI)

Interested in publishing with us?
Contact book.department@intechopen.com

Numbers displayed above are based on latest data collected.
For more information visit www.intechopen.com

3

Data Fusion Performance Evaluation for Dissimilar Sensors: Application to Road Obstacle Tracking

Blanc Christophe, Checchin Paul, Gidel Samuel and Trassoudaine Laurent
LASMEA - Blaise Pascal University
France

1. Introduction

Many science and engineering applications require hardware and software systems that acquire, process, and integrate information gathered by various knowledge sources. A typical example is that of an intelligent road vehicle using several sensors installed in its front bumper to perform a robust driving assistance under all operative conditions. For most of these systems, information made available by the knowledge sources is incomplete, inconsistent, or imprecise. A crucial element in achieving autonomy and efficiency for these systems is the availability of a mechanism that can model, fuse, and interpret the information for knowledge assimilation and decision making. The fused data reflects not only information generated by each knowledge source, but also information that cannot be inferred by either knowledge source acting alone.

This chapter deals with fusing data from sensors that provide information about kinematics characteristics of targets in a moving road scene. The sensors include radar and laser range finder. Information about the positions and velocities, in addition to errors associated with sensor readings is used to solve the target tracking problem. Target tracking with both single and multiple sensors involve this concept: if the track kinematic estimate errors are small, it is easy to locate the next target measurement and continue to update and/or refine the kinematic estimate. The correctly associated measurements provide a "restoring force" since they must correspond to the same underlying target. Loss of accuracy for any reason makes it more difficult to identify the measurements from the target of interest if other targets are present. The aim of the fusion center is to obtain an estimate of the target kinematic state vector and the accuracy of this state estimate quantified by its error covariance. Estimation fusion can be classified into three categories, depending on which information is available at the fusion center: centralized fusion if all measurements are available at the fusion center, decentralized fusion if local estimates are available at the fusion center and hybrid fusion if available information includes both unprocessed data from one sensor and processed data from the other one. In order to be robust, the best achievable performance has to be defined. It depends on the accuracy of the measurements, the sampling interval, and the scenario used. For a linear and Gaussian system, the Kalman filter estimation is optimal. However, in non-linear cases, one cannot conclude on the

Source: Sensor and Data Fusion, Book edited by: Dr. ir. Nada Milisavljević,
ISBN 978-3-902613-52-3, pp. 490, February 2009, I-Tech, Vienna, Austria

optimality of an estimation system. Some comparisons using bounds are thus made to characterize performance limitations, and consequently, to determine whether imposed performance requirements are realistic or not. In time-invariant statistical models, a commonly used lower bound is the Cramer-Rao Lower Bound (CRLB), given by the inverse of the Fisher information matrix. An extension of the CRLB to random parameters was derived: Posterior CRLB (PCRLB). More recently, a simple and straightforward derivation of the PCRLB for the problem of discrete-time nonlinear filtering has been proposed. Many bound comparisons will be made according to fusion architectures, to the accuracy of measurements, to various sensor configurations, and to the scenarios used in order to select the most robust fusion system which has to be installed in our experimental vehicle (VELAC: LASMEA's experimental vehicle). This paper starts with a description of the motivation to use a combination of range-only measurements with Cartesian ones, and provides a mathematical formulation of the problem. Subsequently, the Posterior Cramer-Rao Lower Bounds (PCRLB) are derived and analyzed from the aspect of algorithm convergence. Section 4 presents the two proposed algorithms and their error performance comparison according to the theoretical bounds. Since the combination of range-only measurements with Cartesian ones can be formulated as a nonlinear filtering problem, the Extended Kalman Filter (EKF) and the Particle Filter (PF) are selected as approximation to the optimal recursive Bayesian solution of the nonlinear filtering problem. Finally, an experiment is made in order to evaluate the decentralized fusion performance.

2. Problem description

2.1 Background

Among the mobile robotic problems, obstacle detection and avoidance are the most important. Indeed, each mobile robot having to move in an unknown environment must be able to detect obstacles. J. Hancock's point of view (Hancock, 1999) is that the problem of obstacle avoidance will never be solved. Indeed, mobile robots are becoming more and more capable, and are evolving with increasing speed; these robots will thus need to observe farther and higher areas. Our proposed method for road obstacle detection and tracking combines two dissimilar sensor measurements to achieve a robust performance. It uses a laser based 3D-sensor (Laser Mirror Scanner LMS-Z210-60 from Riegl) which measures range and angles, combined with a radar sensor which delivers range and range rate. For the laser sensor, since target motion is best described in Cartesian coordinates but measurements are available in sensor coordinates, a commonly used method is to convert measurements from sensor to Cartesian coordinates (Li & Jilkov, 2001). Thus, we combine Cartesian target coordinates x and y with radar range r and radar range rate $\dot{r}$ target measurements. Given the characteristics of the radar sensors (Blanc et al., 2004) we can affirm that radar data are complementary with all the other data. Indeed, the radar is insensitive to atmospheric conditions, thus it is judicious, even essential, to use such a sensor for obstacle detection in road environment. These sensors are installed in VELAC (LASMEA's Experimental Vehicle), see Fig. 1.

Lidar sensor : the 3D-Laser Mirror Scanner LMS-Z210-60 is a surface imaging system based upon accurate distance measurement by means of electro-optical range measurement and a two axis beam scanning mechanism. The range finder system is based upon the principle of time-offlight measurement of short laser pulses in the infrared wavelength region. Many methods for time-of-flight's calculation are described in (Hancock, 1999). The task of the

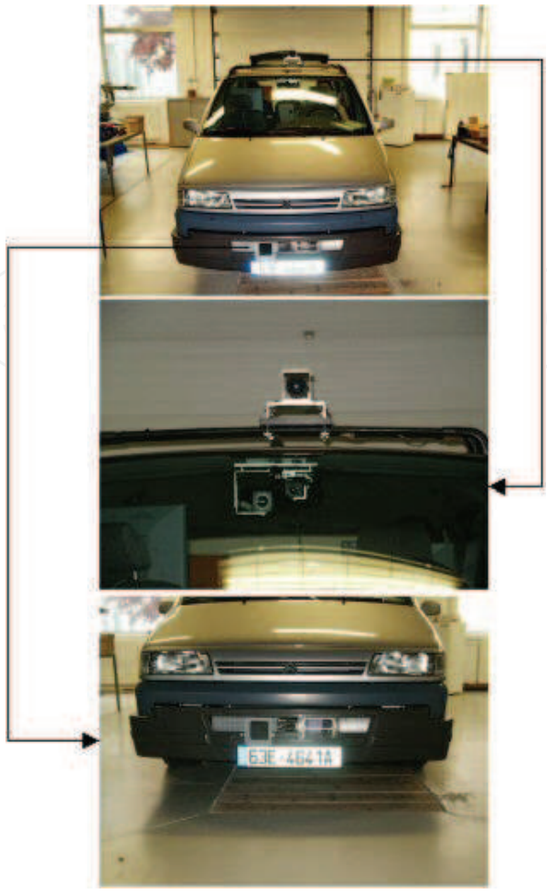

Fig. 1. LASMEA's experimental vehicle exteroceptive sensors.

scanner mechanism is to direct the laser beam for range measurement in an accurately defined position. The 3D images are configurable. In our approach 20 lines x 103 pixels images at nearly 2 Hz are used (see Fig.2). The line scan mechanism (rotating polygonal four facets mirrors) provides a scan angle range about 60° fixed at a speed of 5 lines/s up to maximum 90 lines/s with an angle step width included between 0.072° and 0.36° and a readout accuracy of 0.036°.The frame scanner mechanism which is slower (1°/s up to max 20°/s) than the line scan relies on rotating the optical head together with the fast line scan. This is accomplished by mounting both the line scanner mechanism and the optical head on a rotating table (0° up to max. 333°). The angle step width is 0.072° to 0.36° with an angle readout accuracy of 0.018°. For the obstacle detection, a two parts detection algorithm is used: first the segmentation of the 3D image in regions and second the recognition of the obstacle (particularly road vehicles) among these regions. A region growing algorithm is used to perform the segmentation of the 3D image. A region, including shots located at nearly the same distance d with a tolerance Δd, is parameterized by a vector which includes the size of the target and the position of target's center in the laser scanner reference. These characteristics are then compared to a car model. If parameters of a region are close to those of the model, this region is declared as an obstacle. Finally, a measurement vector $z^{(c)} = \begin{pmatrix} x^{(c)} \\ y^{(c)} \end{pmatrix}$ and its associated covariance $R^{(c)} = \begin{pmatrix} \sigma^2_{x^{(c)}} & 0 \\ 0 & \sigma^2_{y^{(c)}} \end{pmatrix}$ are constructed.

After detection of different obstacles, we are able to track them in consecutive frames using a constant velocity Kalman filter and a nearest neighbor standard data association method. Each target is characterized by a state vector $x^{(c)}$ and its associated covariance $P^{(c)}$. It is noticed that we are able to detect and track several types of obstacles (cars and trucks) (Blanc et al., 2005). The data association system based on research of nearest neighbor seems sufficient for this system. It is thus not necessary to use methods of type JPDAF or with multiple assumptions. Moreover, the precision of the lidar measures allows data association to easily integrate observation which corresponds best to the considered track. We will be able, for example, to use the obstacle size as one of the criteria of associations if several measurements fall into the validation window. The advantage of this method is based on the measurements precision delivered by the lidar and on a high detection probability. Moreover, in a road context, the number of tracks to follow in front of our experimental vehicle is weak. That reduces considerably necessary calculations to the data association systems.

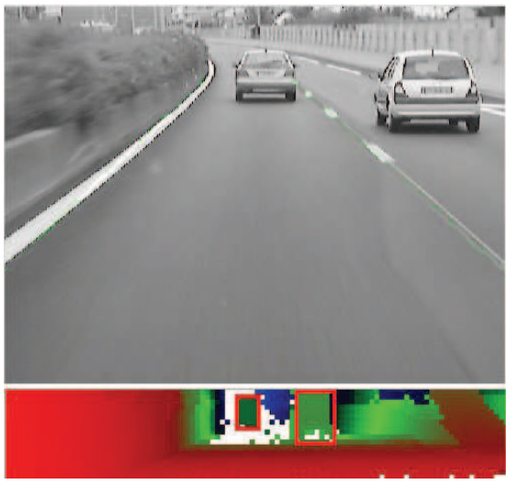

Fig. 2. 3D image and obstacle detection

Radar sensor: the key interests to use a Radar in this project are on the one hand the accuracy of the obstacle speed estimate and on the other hand the quality of its information up to 150 m in spite of difficult weather conditions.
Firstly, the radar data are treated to determine the distance and the relative speed of the objects (or obstacles) located in the enlightened space by the Radar beam. The reader can refer to (Blanc et al., 2004) for many details on the radar data processing. Every 8 ms the radar delivers a measurement of time, amplitude, range and an index speed for all echoes. The range gate is $\delta R = 22.5$ m and an index speed corresponds to a speed of $\delta v = 0.238$ m/s. In radar measurements, one target can generate several echoes in close range gate as well as neighbor speed samples. A pretreatment is thus necessary in order to gather the echoes emanating from the same target. In a second step, a measurement vector $z^{(r)} = \begin{pmatrix} r^{(r)} \\ \dot{r}^{(r)} \end{pmatrix}$ and its covariance matrix $R^{(r)} = \begin{pmatrix} \sigma^2_{r^{(r)}} & 0 \\ 0 & \sigma^2_{\dot{r}^{(r)}} \end{pmatrix}$ are associated to each resulting target.
The Radar tracking is based on Kalman filter and yields to a more accurate range estimate than the gate value (22.5 m) (see Fig. 3). Each target is characterized by a state vector $x^{(r)}$ and its associated covariance $P^{(r)}$.

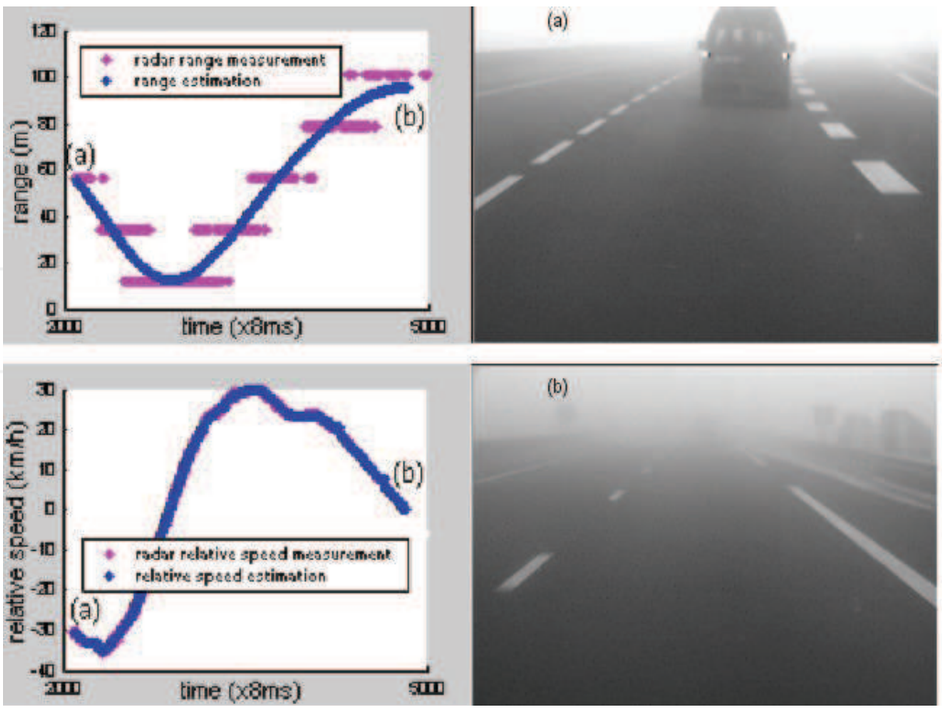

Fig. 3. Radar tracking results in foggy conditions

Obviously, all the sensors have different sample rates. Hypotheses made in this paper are:

- sensors are synchronous
- radar sample rate T_r is lower or equal to the other one T_c (lidar), e.g $T_c = n \times T_r$ with $n \in N^+$;

Moreover, to avoid an additional level of complexity due to false detections and multiple target scenarios, we assume:

- unity probability of detection and zero probability of false alarm;
- all sensor measurements are associated for each target: we don't address the problem of data association.

Thus, the aim of the fusion center is to estimate Cartesian target state X and $P = cov(X)$, its associated covariance, with respect to every T_r, using all available information Y. Estimation fusion can be classified into three categories, depending on which information is available at the fusion module (Li et al., 2003):

- $Y = \left\{\left\{z^{(c)}, R^{(c)}\right\}, \left\{z^{(r)}, R^{(r)}\right\}\right\}$: centralized fusion (CF) if all measurements are available at the fusion center.
- $Y = \left\{\left\{x^{(c)}, P^{(c)}\right\}, \left\{x^{(r)}, P^{(r)}\right\}\right\}$: decentralized fusion (DF) if local estimates are available at the fusion center
- hybrid fusion if available information at the fusion center includes both unprocessed data from one sensor and processed data from the other one.

In this chapter, we focus on centralized and decentralized fusion.

Moreover, between two available Cartesian measurements, the problem can be seen as a problem of target tracking with range-only measurements, i.e. range and range rate measurements. According to our bibliographical research, few publications are devoted to

this problem (Song, 1999) (Ristic et al., 2002). In (Song, 1999) the author discusses the conditions for target observability from range-only measurements. He concludes the same condition as the observability criterion for the related and extensively studied problem of bearing-only target motion analysis: if the target is moving at a constant velocity, the observer must be moving with a non-zero acceleration or if the target is moving at a constant acceleration, the observer must be moving with a non-zero jerk in order to observe the target. In (Ristic et al., 2002), the authors show that, for a typical scenario, tracking algorithms based on range and range-rate measurements can converge toward a steady state.

2.2 Mathematical formulation

Let us consider the fusion target state vector:

$$X = (x, \dot{x}, y, \dot{y})^t \tag{1}$$

where x, y are the tracked positions in the reference frame which is common to both sensors, and $\dot{x}, \dot{y}$ the tracked relative speed. Evolution model can be represented in a matrix form by:

$$X_{k+1} = F_k X_k + G_k V_k, G_k V_k \sim N(0, Q_k) \tag{2}$$

where $F_k$is the transition matrix which models the evolution of X_k, and Q_k the covariance matrix of V_k which represents the acceleration.

$$F_k = \begin{pmatrix} 1 & t_k & 0 & 0 \\ 0 & 1 & 0 & 0 \\ 0 & 0 & 1 & t_k \\ 0 & 0 & 0 & 1 \end{pmatrix}, Q_k = G_k \begin{pmatrix} \sigma_{ax}^2 & 0 \\ 0 & \sigma_{ay}^2 \end{pmatrix} G_k^t, G_k = \begin{pmatrix} \frac{t_k^2}{2} & 0 \\ t_k & 0 \\ 0 & \frac{t_k^2}{2} \\ 0 & t_k \end{pmatrix} \tag{3}$$

The available information at time t_k is defined by:

- Centralized fusion:
  if $z^{(c)}$ is available, i.e. $t_k = n \times T_c$

$$z_k = \begin{pmatrix} z^{(c)} \\ z^{(r)} \end{pmatrix} = \begin{pmatrix} x_k^{(c)} \\ y_k^{(c)} \\ r_k^{(r)} \\ \dot{r}_k^{(r)} \end{pmatrix} = h^{CF}(X^k) + w_k^{CF} = \begin{pmatrix} h_x(X_k) \\ h_y(X_k) \\ h_r(X_k) \\ h_{\dot{r}}(X_k) \end{pmatrix} + w_k^{CF}, w_k^{CF} \sim N(0, R_k^{CF}) \tag{4}$$

$$R_k^{CF} = \begin{pmatrix} R_k^{(c)} & 0 \\ 0 & R_k^{(r)} \end{pmatrix} \tag{5}$$

else

$$z_k = (z^{(r)}) = \begin{pmatrix} r_k^{(r)} \\ \dot{r}_k^{(r)} \end{pmatrix} = h^{CF}(X^k) + w_k^{CF} = \begin{pmatrix} h_r(X_k) \\ h_{\dot{r}}(X_k) \end{pmatrix} + w_k^{CF}, w_k^{CF} \sim N(0, R_k^{CF}) \tag{6}$$

$$R_k^{CF} = \left(R_k^{(r)}\right) \tag{7}$$

- Decentralized fusion
  if $x^{(c)}$ is available, i.e. $t_k = n \times T_c$

$$z_k = \begin{pmatrix} x^{(c)} \\ x^{(r)} \end{pmatrix} = \begin{pmatrix} \tilde{x}_k \\ \tilde{\dot{x}}_k \\ \tilde{y}_k \\ \tilde{\dot{y}}_k \\ \tilde{r}_k \\ \tilde{\dot{r}}_k \end{pmatrix} = h^{DF}(X^k) + w_k^{DF} = \begin{pmatrix} h_x(X_k) \\ h_{\dot{x}}(X_k) \\ h_y(X_k) \\ h_{\dot{y}}(X_k) \\ h_r(X_k) \\ h_{\dot{r}}(X_k) \end{pmatrix} + w_k^{DF}, w_k^{DF} \sim N(0, R_k^{DF}) \tag{8}$$

$$R_k^{DF} = \begin{pmatrix} P_k^{(c)} & P_k^{(cr)} \\ P_k^{(cr)} & P_k^{(r)} \end{pmatrix} \tag{9}$$

where $P_k^{(cr)}$ is the cross covariance matrix
else

$$z_k = (x^{(r)} = \begin{pmatrix} \tilde{r}_k \\ \tilde{\dot{r}}_k \end{pmatrix} = h^{DF}(X^k) + w_k^{DF} = \begin{pmatrix} h_r(X_k) \\ h_{\dot{r}}(X_k) \end{pmatrix} + w_k^{DF}, w_k^{DF} \sim N(0, R_k^{DF}) \tag{10}$$

$$R_k^{DF} = \left(P_k^{(r)}\right) \tag{11}$$

$$\begin{cases} h_x(X_k) = x_k \\ h_{\dot{x}}(X_k) = \dot{x}_k \\ h_y(X_k) = y_k \\ h_{\dot{y}}(X_k) = \dot{y}_k \\ h_r(X_k) = \sqrt{x_k^2 + y_k^2} \\ h_{\dot{r}}(X_k) = \dfrac{x_k^2 \dot{x}_k^2 + y_k^2 \dot{y}_k^2}{\sqrt{x_k^2 + y_k^2}} \end{cases} \tag{12}$$

3. Posterior Cramer-Rao lower bounds

3.1 Derivation of the bounds

The system defined by both the evolution and the measurement model, respectively defined in (2) and (4,5) is considered. If $\hat{X}_{k/k}$ is an unbiased estimator of X_k, calculated from the measurement sequence $Z_k = \{z_1, \cdots, z_k\}$ and from the knowledge of $p(X_0)$ (initial pdf), then the covariance matrix of $\hat{X}_{k/k}$, noted $P_{k/k}$ admits a lower bound given by:

$$P_{k/k} \triangleq E\{(\hat{X}_{k/k} - X_k)(\hat{X}_{k/k} - X_k)^t\} \geq J_k^{-1} \tag{13}$$

where J_k is the Fisher information matrix which we want to determine. Tichavsky et al. (Tichavsky et al., 1998) proposed a method to calculate J_k recursively:

$$J_{k+1} = D_k^{22} - D_k^{21}(J_k + D_k^{11})^{-1}D_k^{12} \tag{14}$$

where since the evolution model is linear and noises are Gaussian:

$$D_k^{11} = F_k^t Q_k^{-1} F_k \tag{15}$$

$$D_k^{12} = -F_k^t Q_k^{-1} = [D_k^{21}]^t \tag{16}$$

$$D_k^{22} = \begin{cases} Q_k^{-1} + E\left\{\left[\tilde{H}_{k+1}^{CF}\right]^t \left[R_{k+1}^{CF}\right]^{-1} \tilde{H}_{k+1}^{CF}\right\} \; if \; CF \\ Q_k^{-1} + E\left\{\left[\tilde{H}_{k+1}^{DF}\right]^t [R_{k+1}^{DF}]^{-1} \tilde{H}_{k+1}^{DF}\right\} \; if \; DF \end{cases} \tag{17}$$

where $\tilde{H}_{k+1}^{CF}$ and $\tilde{H}_{k+1}^{DF}$ are respectively the Jacobian matrix of $h_{k+1}^{CF}(X_k)$ and $h_{k+1}^{DF}(X_k)$ evaluated at the true value of X_{k+1}. Finally, by using the inversion matrix lemma, the recursive information matrix calculation is:

$$J_{k+1} = (Q_k + F_k J_k^{-1} F_k^t)^{-1} + \begin{cases} E\left\{\left[\tilde{H}_{k+1}^{CF}\right]^t \left[R_{k+1}^{CF}\right]^{-1} \tilde{H}_{k+1}^{CF}\right\} if \; CF \\ E\left\{\left[\tilde{H}_{k+1}^{DF}\right]^t [R_{k+1}^{DF}]^{-1} \tilde{H}_{k+1}^{DF}\right\} if \; DF \end{cases} \tag{18}$$

In practice, the most difficult problem is the calculations of the expected value operator E in (18). The expectation is only taken with respect to the state vector X_k (the bound is independent of the actual measurement sequence). A Monte Carlo approximation can be applied to implement the theoretical PCRB formulae. One first needs to create a set of state vector realizations, the so-called target trajectories. Then the appropriate term in (12) is computed as the average over this set.

The recursions start with the initial information matrix J_0 computed from the initial density $p(X_0)$. If $p(X_0)$ is Gaussian then $J_0 = P_0^{-1}$ else $J_0 = E\left\{\Delta_{X_0}^{X_0} \log p(X_0)\right\}$.

3.2 Analysis of the bounds

The scenario used is constructed from a ground truth approximation. It is a typical case of adaptive cruise control (ACC) scenario. For this, VELAC and only one obstacle are equipped with DGPS. Their locations are acquired every second. Obstacle position is sent to VELAC by MF communications. Relative positions and velocities are shown in Fig. 4 after approximation. VELAC and obstacle move at a speed bounded by 20km/h and 90km/h.

As described in (Blanc et al., 2007) it is not necessary to stack r in the Z_k measurement vector except if $\sigma_r \ll \sigma_x, \sigma_y$ (with our sensors $\sigma_r > \sigma_x, \sigma_y$). Firstly, the Fig. 5 confirms, as expected, that the more data are available the more performance increases. As we can see, PCRLBs of x and $\dot{x}$ increase between two Cartesian measurements as it the trajectory taken does not respect the observability criterion. For the calculations 100 MC runs are used and $R^{(c)} = \begin{pmatrix} 2^2 & 0 \\ 0 & 2^2 \end{pmatrix}$, $R^{(r)} = \begin{pmatrix} 7^2 & 0 \\ 0 & 0.2^2 \end{pmatrix}$. Moreover, decentralized and centralized estimation fusion architectures have an equivalent good performance for this ACC scenario.

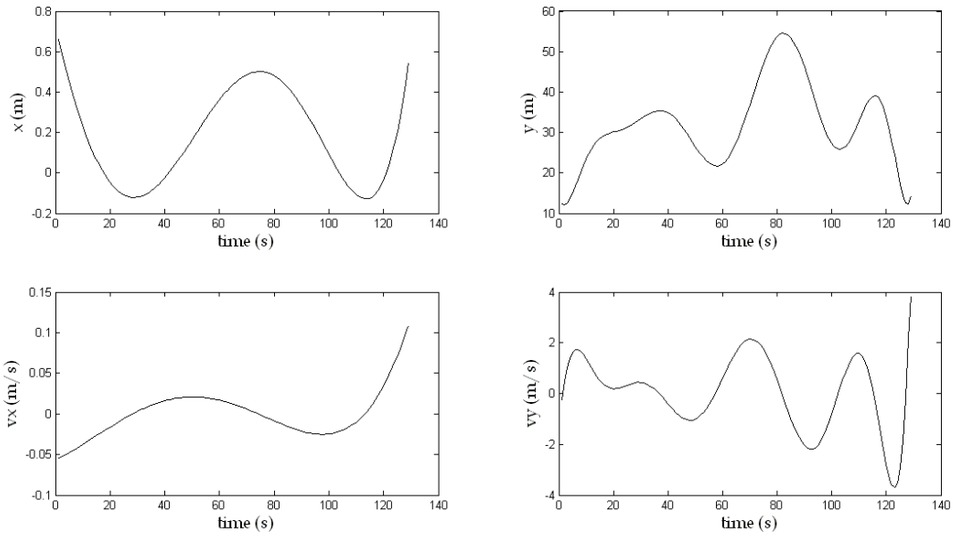

Fig. 4. A scenario used for the analysis of Posterior Cramer-Rao lower bounds

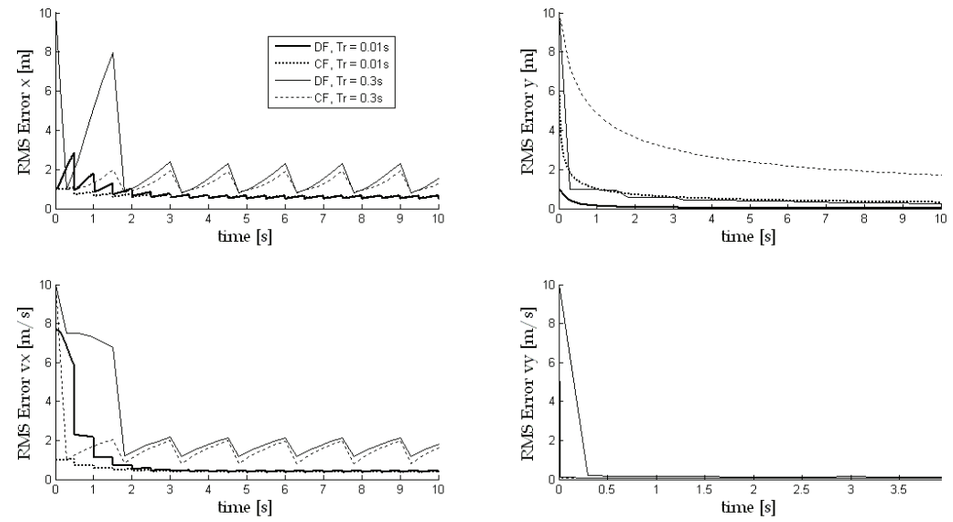

Fig. 5. Decentralized fusion (solid line) and centralized fusion (dashed line) PCRLB of $x, \dot{x}, y, \dot{y}$ with a fixed $T_c = 0.5\ s$, a varying $T_r = 0.01\ s, 0.3\ s$

4. Tracking algorithms

4.1 Extended Kalman filter

Estimation fusion using range, range-rate and Cartesian measurements, is a non-linear dynamic state estimation problem because the measurement equation is non-linear (12). The Kalman filter is therefore inappropriate. The conventional approach is to approximate Eqs. (4, 6, 8, 10) by a series expansion and then to use an equivalent measurement matrix in the ordinary Kalman filter equations: Extended Kalman filter (EKF) for a first-order series

expansion (linearization) of the non-linear measurement equation. The recursive equations of the EKF are presented below to describe the evaluation of the relative estimated state $X_{k+1/k+1}$ and its associated covariance matrix $P_{k+1/k+1}$ by using the measurement z_k and the relative state vector $X_{k/k}$ with its associated covariance matrix $P_{k/k}$. The state equation prediction is worked out by Eq. (2) while the covariance matrix is given by:

$$P_{k+1/k+1} = F_k P_{k/k} F_k^t + G_k Q_k G_k^t \tag{19}$$

The measurement prediction is given by Eqs. (4, 6, 8, 10). We don't stack r in the measurement vector for Eqs. (4, 8) as it is proposed in previous section.
The Kalman gain matrix can be evaluated as

$$K_{k+1}^m = P_{k+1/k+1}(H_{k+1}^m)^t \left[H_{k+1}^m P_{k+1/k+1}(H_{k+1}^m)^t + R_{k+1}^m\right]^{-1} \tag{20}$$

where m represents CF or DF, and H_{k+1}^m is the linearised measurement matrix evaluated at the predicted state.
Finally, the updated fusion state and its associated covariance matrix are given by:

$$X_{k+1}^m = X_{k+1/k}^m + K_{k+1}^m \left(z_{k+1} - h^m(X_{k+1/k}^m)\right) \tag{21}$$

$$P_{k+1}^m = (I - K_{k+1}^m H_{k+1}^m) P_{k+1/k}^m \tag{22}$$

4.2 Particle filter

Originally developed in the tracking community (Gordon et al., 1993), the particle filtering is currently enjoying a strong development in many research fields (vision, localization, navigation, robotics, etc.), in particular in multi-target tracking. This filter is a sequential Monte-Carlo method in which particles traverse the state space in an independent way, and interact under the effect of a probability function which automatically concentrates the particles in the state space areas of interest. This method has the advantage of not requiring linear or Gaussian assumptions on the model. Moreover, it is very easy to implement, since it is enough to know how to simulate independent various trajectories of the model. We propose here, to carry out a particle filtering on the fusion module level. A fusion state is initialized. From this vector, a set of N_s particles is built. Noise particles are generated $(B_O^{(i)}, i = 1, .., N_s)$ and applied to the initial vector:

$$X_{0/0}^{m^{(i)}} = X_{0/0}^m + B_O^{(i)}, \forall i \in [1 \cdots N_s] \tag{23}$$

Then, the model defined in (2) is applied to N_S particles in a prediction step. Correction is carried out on the level of the calculation of the weights. We calculate N_s weights assigned to the N_s predicted particles. We have:

$$w_k^{m^{(i)}} = \mathrm{p}(\mathrm{z_k}/\mathrm{X_{k/k-1}^{m(i)}}) \tag{24}$$

Weights are then normalized, and finally the fused state considered is given by:

$$X_k^m = \sum_{i=1}^{N_s} w_k^{m^{(i)}} \mathrm{X_{k/k-1}^{m(i)}} \tag{25}$$

and its covariance by:

$$P_k^m = \sum_{i=1}^{N_s} w_k^{m(i)} \left(\mathrm{X}_{\mathrm{k/k-1}}^{\mathrm{m(i)}} - X_{k/k-1}^m\right)\left(\mathrm{X}_{\mathrm{k/k-1}}^{\mathrm{m(i)}} - X_{k/k-1}^m\right)^{\mathrm{t}} \tag{26}$$

The particles are resampled and returned to the prediction step.

4.2 Algorithm performance and comparison

The performance of estimation fusion for two algorithms is analyzed by Monte-Carlo simulations. The analysis is made for the trajectory presented in Fig. 4. The measurement covariances are assumed to be $R^{(r)} = diag[7^2, 0.2^2]$ and $R^{(c)} = diag[2^2, 2^2]$.
The sampling rates are $T_r = 0.01\ s$ and $T_c = 0.5\ s$. The resulting error curves were computed to the theoretically derived PCRLB. The estimation error is defined as $e_k = X_k^m - X_k$. The performance is measured by the root mean square error (RMSE), which, for component j of the state vector, is defined as $\sigma_{e_k}^j = \sqrt{E\left(e_k^{j\,2}\right)}$ where the expectation operator was computed by averaging over 50 independent Monte-Carlo runs. Results are shown in Fig. 6.

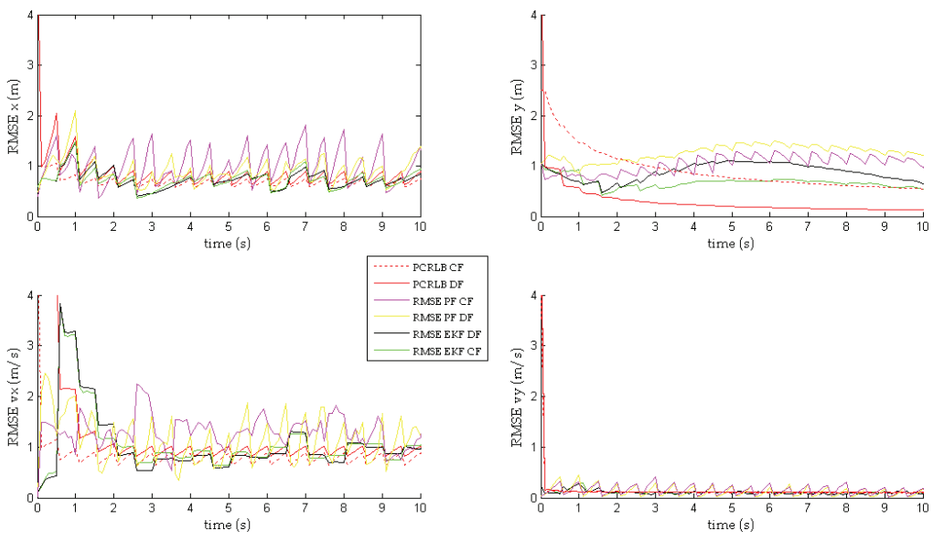

Fig. 6. Performance of EKF and PF against PCRLB

Firstly, we may notice that the EKF and particle filter errors are initially smaller than the square root of PCRLB which is unexpected. This result is due to the initialization, which does not exactly match to the inverse of the initially used information matrix in the PCRLB computation. For clarity, results for particle filter are present only with 2000 particles. Nevertheless, we observe that as the number of particles is increased, the performance of the particle filters improves, and approaches the PCRLB's. This improved accuracy of the particle filter, however, is at the expense of the computational load. Particle filter with 10000 particles is equivalent to EKF. Thus, in practical operation system, the EKF appears more suitable for implementation than the particle filter.

5. Experiments

Quantitative results for decentralized fusion are obtained with a ground truth. Velac and only one obstacle are equipped with DGPS. Their locations are acquired every second. Obstacle position is sent to Velac by MF communication. In the same time, the obstacle is tracked by both processes (Radar/Lidar). Decentralized fusion process and comparison are done offline. The measurement system includes a differential GPS Omnistar which delivers trames with format TSIP (Trimble Standard Interface Protocol). This GPS gives, in the best configuration, a position with a ±40 cm accuracy. It delivers a coefficient, called gdop: the current accuracy is gdop times 40 cm. DGPS errors are shown in Fig. 7. Moreover, for data communication, a radio modem of Satel receives trames coming from the obstacle. Fig. 7 shows the results for the range estimation by extended Kalman filter and particle filter. Moreover, it shows the radar and lidar estimate. We see that radar estimate is less accurate than lidar estimate in this particular scenario. The DGPS reference allows computing root mean square error and its standard deviation (std) for both filters. As it is shown on results, performance of range estimation is correct for both filters. Errors and DGPS accuracy have almost the same order. Moreover, as expected, the EKF have very small computation time compared with the particle filters. Only EKF allows real time utilization because of the radar data rate which is 8 ms.

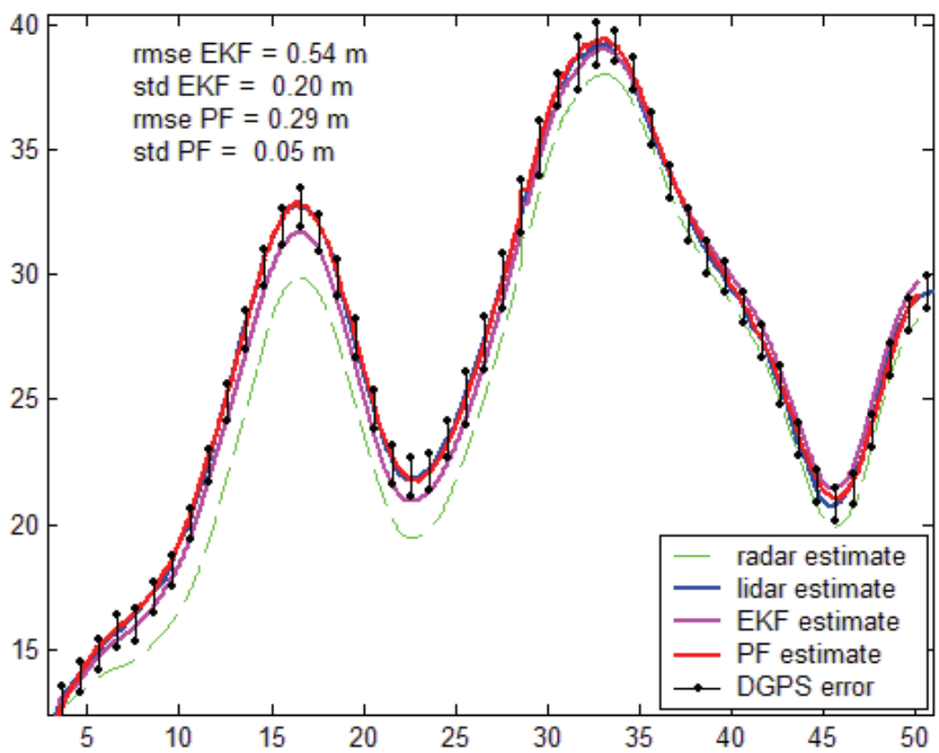

Fig. 7. Range estimation by EKF and particle filter

6. Conclusion

This paper has discussed the problem of centralized/decentralized fusion estimation for target tracking using range, range-rate and Cartesian measurements for road obstacle tracking. The Posterior Cramer-Rao Lower Bounds were derived and two tracking algorithms were developed. The PCRLBs allow us to predict the best achievable performance under various conditions such as the relative target trajectory, and measurement sample rate. Two algorithms have been considered: the extended Kalman filter and the particle filter. This study has shown that both algorithms are efficient for this kind of scenario even if the particle filter is unattractive for implementation in a practical operational system. Our future work will consist in developing a new method of laser/camera fusion for pedestrian detection. This work will take place in the context of the LOVe (Logiciel d'Observations des Vulnérables) which aims at improving road safety, mainly focusing on pedestrian security.

7. References

Blanc, C. ; Aufrère, R. ; Malaterre, L. ; Gallice, J. & Alison, J. (2004). Obstacle detection and tracking by millimetre wave radar, *5th IFAC Symposium on Intelligent Autonomous Vehicles IAV*, Portugal, July 2004, Lisboa

Blanc, C. ; Trassoudaine, L. & Gallice, J. (2005). EKF and particle track-to-track fusion: a quantitative comparison from radar/lidar obstacle tracks, *8th International Conference on Information Fusion*, USA, July 2005, Philadelphia

Blanc, C. ; Checchin, P. ; Gidel, S. & Trassoudaine, L. (2007). Data fusion performance evaluation for range measurements combined with Cartesian ones for road obstacle tracking, *International Conference on Vehicular Electronics and Safety*, China, December 2007, Beijing

Gordon, N.J. ; Salmond, D.J.; Smith, A.F.M. (1993). Novel approach to nonlinear/non-Gaussian Bayesian state estimation. *Radar and Signal Processing, IEE Proceedings F,* Vol. 140, No.2, (April 1993) 107-113, ISSN 0956-375X.

Hancock, J. (1999). Laser Intensity-Based Obstacle Detection and Tracking, *PhD Thesis*, Carnegie Mellon University, The Robotics Institute

Li, X.R. & Jilkov, V.P. (2001). A Survey of Manoeuvring Target Tracking Part III, *Proceedings of SPIE Conference on Signal and Data Processing of Small Targets*, USA, July-August 2001, San Diego

Li, X.R.; Yunmin, Z. ; Jie, W. & Chongzao, H. (2003). Optimal linear estimation fusion .I. Unified fusion rules**.** *IEEE Transactions on Information Theory,* Vol.49, No.9, (September 2003) 2192-2208, ISSN 0018-9448

Ristic, B.; Arulampalam, S. & Mccarthy, J.(2002). Target motion analysis using range-only measurements: algorithms, performance and application to ISAR data. *Signal Processing*, Vol. 82, No.2, (February 2002) 273-296, ISSN 0165-1684

Song, T.L. (1999). Observability of target tracking with range-only measurements. *IEEE Journal of Oceanic Engineering,* Vol. 24, No.3, (July 1999) 383-387, ISSN 0364-9059.

Tichavsky, P.; Muravchik, C.H. & Nehorai, A. (1998).Posterior Cramer-Rao bounds for discrete-time nonlinear filtering. *IEEE Transactions on Signal Processing*, Vol. 46, No.5, (May 1998) 1386-1396, ISSN 1053-587X.

Sensor and Data Fusion

Edited by Nada Milisavljevic

ISBN 978-3-902613-52-3
Hard cover, 436 pages
Publisher I-Tech Education and Publishing
Published online 01, February, 2009
Published in print edition February, 2009

Data fusion is a research area that is growing rapidly due to the fact that it provides means for combining pieces of information coming from different sources/sensors, resulting in ameliorated overall system performance (improved decision making, increased detection capabilities, diminished number of false alarms, improved reliability in various situations at hand) with respect to separate sensors/sources. Different data fusion methods have been developed in order to optimize the overall system output in a variety of applications for which data fusion might be useful: security (humanitarian, military), medical diagnosis, environmental monitoring, remote sensing, robotics, etc.

How to reference

In order to correctly reference this scholarly work, feel free to copy and paste the following:

Blanc Christophe, Checchin Paul, Gidel Samuel and Trassoudaine Laurent (2009). Data Fusion Performance Evaluation for Dissimilar Sensors: Application to Road Obstacle Tracking, Sensor and Data Fusion, Nada Milisavljevic (Ed.), ISBN: 978-3-902613-52-3, InTech, Available from: http://www.intechopen.com/books/sensor_and_data_fusion/data_fusion_performance_evaluation_for_dissimilar_sensors__application_to_road_obstacle_tracking

INTECH
open science | open minds

InTech Europe
University Campus STeP Ri
Slavka Krautzeka 83/A
51000 Rijeka, Croatia
Phone: +385 (51) 770 447
Fax: +385 (51) 686 166
www.intechopen.com

InTech China
Unit 405, Office Block, Hotel Equatorial Shanghai
No.65, Yan An Road (West), Shanghai, 200040, China
中国上海市延安西路65号上海国际贵都大饭店办公楼405单元
Phone: +86-21-62489820
Fax: +86-21-62489821

IntechOpen